LEAPING IN LOW GRAVITY

Modeling MASCOT's hopping locomotion on asteroid Ryugu

R. Lichtenheldt*, J. Reill**

*German Aerospace Center, Institute of System Dynamics and Control, DLR, Germany
e-mail: Roy.Lichtenheldt@dlr.de

**German Aerospace Center, Institute of Robotics and Mechatronics, DLR, Germany

Abstract

DLR's lander MASCOT is an innovative system to explore and traverse asteroid surfaces. Launched piggyback on JAXA's Hayabusa II spacecraft in December 2014, MASCOT is already on its four years cruise phase to the asteroid Ryugu-1999JU3. Even though MASCOT features a 1-DOF mobility actuator only, it has to deal with the complex interaction of the cuboid lander with the terrain. Thus, a certain orientation of MASCOT cannot be achieved directly. Hence, the mobility unit developed by DLR's Robotics and Mechatronics Center enables MASCOT to up-right to the measurement position and to relocate by hopping motion. In this article, the optimization-based technique used to identify suitable and robust trajectories of the mobility unit is explained and exemplified for hopping and up-righting.

1 INTRODUCTION

The earlier exploration of our solar system mostly focused on our moon and neighboring planets. In contrast asteroids, comets and small planetary bodies in general are not yet well investigated. In the recent time exploration of these bodies has become further demanded and popular (e.g. [1]). MASCOT is DLR's lander [2] on board of JAXA's Hayabusa II mission to Ryugu-1999JU3, launched in December 2014. It is a cuboid system of roughly 10 kg, whereby moret han 35% of this mass is scientific payload. Achieving an exceptionally high payload rate was one of MASCOT's goals right from the beginning. In order to allow the instruments to work, a certain lander orientation needs to be achieved. However, due to low gravity and the resulting bouncing after landing, this posture cannot be achieved directly after landing. Thus MASCOT features a novel locomotion system for hopping and up-righting to measurement position [3]. The locomotion system called mobility unit is an internal controllable rotor with an excentrical rotor mass. As the dependence of the desired hopping trajectory on the motion profile of the mobility unit arm is complex, a suitable trajectory cannot be determined analytically or by experiment in advance. Even in parabolic flight campaigns the low-gravity phases are not sufficiently long for trajectory tuning. As it is not possible to define the trajectories based on real prototyping, a multibody model in conjunction with a mathematical description of the asteroid's terrain geometry and gravity field is developed. Throughout the article the modeling approaches for MASCOT itself as well as the asteroid's model will be explained. The model features a description of MASCOT's kinematics, dynamics and contact mechanics to the asteroid surface in order to rate a-priori created trajectories. Applying the modeling approach to multi-objective optimization allows for the systematic search for suitable trajectories in an automated process. Using the optimization framework MOPS [4] developed by DLR-SR a toolkit for trajectory optimization on low gravity bodies is developed. Throughout the article, the toolkit, the objectives as well as the stepwise optimization approach [5] will be explained. For hopping the optimization based technique is exemplified by finding a trajectory for a maximum hopping distance. For up-righting the most important objectives are short bouncing time and the binary goal, defined by the equilibrium orientation of MASCOT. Nevertheless up-righting needs to be as robust as possible against parameter deviations exerted either by e.g. inhomogeneous regolith or control inaccuracies due to the harsh environmental conditions. Non-robust solutions might cause MASCOT to land on the wrong face and require repeated up-righting and thus shorter periods for the scientific measurements.

2 MASCOT MOBILITY

The mobility subsystem consists of an actuator unit with an excentric arm (MobUnit), a controller and power electronics PCB (MobCon) and an additional hall sensor PCB to detect the reference position of the excentric arm. Fig.1 shows the main components before integration into the MASCOT electronics box. Since most of the scientific instruments operations are dependent on MASCOT's orientation on asteroid surface, the mobility subsystem is very important for mission success. Therefore, every component was realized as redundant as possible. Nevertheless, due to space and weight limitations the up-righting and

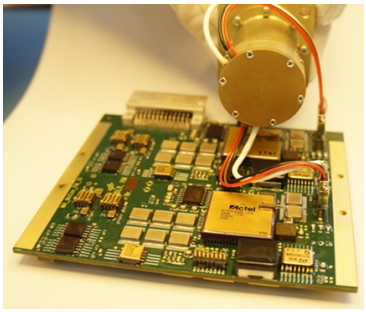

Figure 1. : Flight model photo image that shows mobility motor connected to the controller and power electronics board

hopping maneuvers need to be performed with a single, non-redundant motor. Because of that a brushless DC motor was chosen as it is a reliable and lightweight solution that offers also offers a high peak torque output. This may be helpful to overcome friction and cold welding effects in mechanics as well as to put high jerk to the system if needed. Together with a Harmonic Drive gearing the developed actuator is very compact. Compared to DC motors the brushless DC motor needs less mechanical parts and has no brushes at all. The commutation is realized by power electronics and hall sensor information. The mobil-

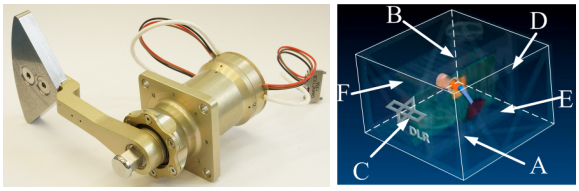

Figure 2. : Flight model photo image that shows mobility motor and the excentric arm (l.), Orientations of MASCOT (r.)

ity electronics is set up completely cold redundant and put on a single PCB. Each redundancy path is able to drive the motor unit even if there might occur a failure in the other path. A special coupling network was developed to connect two power electronics circuits to one single motor [3]. Depending on housekeeping data and error messages the OBC decides which redundancy path is to be used and powered. The communication to OBC, sensor data collection and interpretation, control of motor trajectory, computation of absolute position and safety issues is all handled by a radiation hardened Microsemi FPGA. This FPGA needs to drive the motor power MOSFETs by use of high and low side gate drivers. As the radiation tolerant gate drivers did not fit on the restricted electronics board size an industrial BLDC motor controller was considered. Of course the motor controller has successfully undergone several radiation tests (see [6]) before.

3 MODELING OF THE LOCOMOTION SYSTEM

In order to determine the trajectories for MASCOT's mobility unit, the model previously used to support design decisions described in [7] is enhanced. Therefor not only the lander's system model, but also the description of the asteroid is adapted taking latest findings into account.

3.1 Multibody Model

In order to cover the kinematics and dynamics, MASCOT's mechanical system is modeled using multibody dynamics techniques, implemented in the commercial software SIMPACK. Dependent on the application either pure rigid body models or flexible multibody dynamics based on modal reduction are used. The flexible part is thereby limited to MASCOT's main structural frame, including the electronics box and its interior, but treating the payload and the mobility as pure point masses. The subjacent FEM model [8] is provided by DLR Institute of Composite Structures and Adaptive Systems.

3.2 Contact Dynamics Model

For MASCOT's locomotion, based on hopping and repeated low-energy impact on the asteroid's surface, understanding the corresponding contact dynamics is crucial. Yet, the knowledge on Ryugu and asteroids in general is limited. Thus without detailed knowledge, complex models do not add beneficial detail to the simulation. For that reason contact dynamics between the lander and the asteroid has been modeled simplified as a visco-elastic surface model. The nominal parameters, i.e. Young's Modulus E and Poisson's ratio ν, have been determined in [7] and improved during the mission development phase. The contact dynamics are based on SIMPACK's Polygonal Contact Model (PCM), enhanced by special approaches for parameter estimation. Thereby the latest improvement bases on usage of the correlation between coefficient of restitution ε_r and critical damping k_{krit} to identify the damping of an impacting body by [9] and the extension by [10]:

$$k = \frac{2 \cdot |\ln(\varepsilon_r)|}{\sqrt{\ln(\varepsilon_r)^2 + \pi^2}} \cdot \sqrt{\frac{m \cdot r_c \cdot E}{3(1-\nu^2)} \sqrt{|u_0|}} \qquad (1)$$

where m is the mass of the lander, r_c the equivalent contact radius for non-spherical bodies and u_0 the allowed relative overlap. As the underlying assumptions by Lichtenheldt have been originally made for particle systems and stiff contacts [11], the approach is slightly adapted and coefficients of restitution based on experimental data are used for the contact between soil and the lander. Concluding a range of $\varepsilon_r \in [0.2; 0.3]$ is found for granular soils.

3.3 Asteroid Model

In order to describe MASCOT's locomotion on the asteroid, a model of the latter is needed. This model includes the surface description, as well as the correspondent gravity field and assumptions regarding the asteroid body. Such are assumptions on the density and homogeneity of the planetary body and its motion behavior. For the final trajectories, which will be used in the mission operations, a farther detailed asteroid model including rotation, shape, gravity field and surface is needed. Therefore, the landing site has to be known, in order to find suitable trajectories for the respective region, as different regions will feature different gravity and environment. Additionally, with increasing model complexity, comparability and interpretability of the optimization results decrease. This phenomenon is due to effects exerted by gravity potential and others. Thus for the evaluation of the optimization-based trajectory identification strategy's applicability, a simplified model is used in this article. Simplifications are also applied due to the lack of knowledge on Ryugu's surface at the present time. Anyway, further detailed models for the mission are object to ongoing work.
The simplified model features a spherical shape and homogeneous density. Thus the gravity field is also spherical and its effect on MASCOT is dependent on the height of the center of gravity. The parameters of the spherical body are compiled from the current knowledge on the asteroid, i.e. its assumed size and mass. The asteroid is simplified as a non-rotating body for comparability reasons. As the latter alters the effective escape velocity, MASCOT's velocities are checked throughout the optimization process. Furthermore the asteroid is assumed to have a smooth, homogeneous surface. The surface roughness and texture itself is covered by Coulomb friction. As Hayabusa II approaches Ryugu, all knowledge gathers until landing will be fed into the asteroid model in order to enhance the accuracy of the model. For further detail, the model is already prepared to cover rotating asteroids of arbitrary shape (surface mesh) with elliptical gravity fields [12] solving Legendre's elliptic integral of the second kind.

3.4 Experimental Model Verification

In order to make sure, that the identified trajectories are suitable for MASCOT's mission on Ryugu, the simulation models need to be checked using measurements. Due to the micro-gravity environment on the asteroid, verification on Earth is a demanding task. Thus in order to check the motion itself, parabolic flight campaigns using scaled excentric arm masses have been used. These campaigns showed a good agreement between measured and simulated motion behaviour. Nevertheless, due to the short period of micro-gravity, a full maneuver demonstration of MASCOT was not possible. Hence, to further check

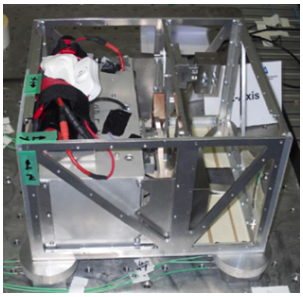

Figure 3. : High-precision measurement of ground reaction forces on four force sensors in terrestrial conditions

the model of MASCOT itself, precision force measurements were taken in terrestrial environmental conditions. The configuration of the test is shown in Fig.3. Once the

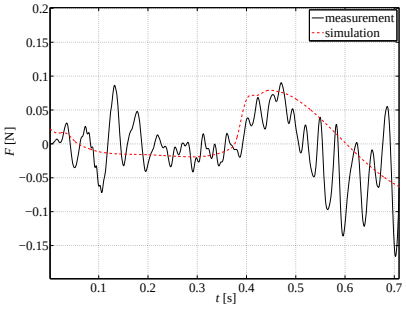

Figure 4. : Comparison of measured and simulated reaction force

MASCOT model is able to correctly simulate the contact forces at various operations of the mobility unit, it is assumed that the model is also able to reproduce the motion behavior in the relevant environment. Fig.4 exemplarily shows the congruence of measured and simulated force signals in the low frequency range of $[3;25]$ Hz, relevant for hopping. Thereby the model computation and storage of results is 10 to 20 times faster than the real motion sequence, hence it results in a real time factor of [0.05,0.1].

4 Optimization-based Approach for Identification of Trajectories

Due to the complex interaction of the lander with the asteroid surface, trajectory determination by model inversion or similar techniques used to implement feed-forward control of the mobility unit are not possible. As manual evaluation of trajectories would end up in long trial & error campaigns, optimization is used to automatically tune the trajectory parameters to the lander's optimal motion behaviour. A trajectory T consists of five parameters:

- start angle of the mobility arm θ_i
- angular acceleration of the motor $a^\mathrm{a}_\mathrm{arm}$

- maximum rotational velocity $\omega_{\max}$
- angular deceleration of the motor $a^{\mathrm{d}}_{\mathrm{arm}}$
- end angle of the mobility arm θ_{e}

$$T = \left\{ \theta_{\mathrm{i}}, \theta_{\mathrm{e}}, a_{\max}, a^{\mathrm{d}}_{\mathrm{arm}}, \omega_{\max} \right\}_{\mathrm{v}} \tag{2}$$

These parameters are then compiled into the class C^1 position function.

4.1 Approach

The basic approach of the optimization based identification of suitable trajectories is to systematically evaluate and rate trajectories by their fitness. This fitness is thereby calculated from several objective functions, based on the simulation results. These objectives will be explained in the correspondent results section for hopping and up-righting. As the knowledge on the shape of the response-surface for the objectives is unknown, genetic algorithms based on evolutionary strategies are applied as the algorithm of choice. While the current knowledge on Ryugu is yet limited, robust solutions, working for a variety of environmental parameters are needed. This robustness of the solution is assured by performance of several parallel simulations per individual of the genetic algorithm. These simulations will be called sub-individuals in this article, as their entity forms one individual. Thereby, the variation of environmental parameters is performed over the discrete sub-individuals. To find robust solutions the mean gradient of the objective J_k over the sub-individuals ς

$$\frac{\mathrm{d}J_k}{\mathrm{d}\varsigma} = \|\nabla J_k\|_1 \tag{3}$$

is performed: Hence low gradients refer to low sensitivity on the parameters and thus a robust solution, whereas a high gradient show a solution sensitive on the varied sub-individual parameters. For the up-righting optimizations, the sub-individuals are divided in ten cases, listed in table 1. Thereby mainly soil parameters are varied in wide ranges, but also deviations in the trajectory itself are used. It shall be mentioned, that these variations are a first set to evaluate the suitability of the approach using worst case assumptions, which might even be worse than the actual variation range on the asteroid. The total optimization statement yields:

$$T' \in \arg\min_{T} \left[J, \|\nabla J_k\|_1 \right] \Leftrightarrow T \wedge \; J(T') \leq J(T) \tag{4}$$
$$\wedge \, \|\nabla J_k(T')\|_1 \leq \|\nabla J_k(T)\|_1; \; \forall \; T' \in D_T \; \wedge \; J_{\mathrm{C}} \equiv 1;$$

4.2 Framework - TOMATO

The approach described above is implemented in the Tool for MASCOT's Arm Trajectory Optimization (TOMATO, see Fig.5) which is based on the optimization framework MOPS [4], both developed by DLR Institute of System Dynamics and Control. TOMATO mainly connects SIMPACK to MOPS and takes over the job scheduling for parallel processing of the sub-individuals including unique naming and management of the results. TOMATO also provides the infrastructure for determination of the objectives based on the time dependent data in a fail safe way. Hence the main focus is to ensure, that long optimization runs will not be aborted by errors in single individuals or sub-individuals in order to allow for full automatization of the process. In order to decrease the time needed to finish optimizations TOMATO allows for multithreading in terms of processing sub-individuals up to the number of cores or licenses available.

5 APPLICATION & RESULTS

In this section results used for verification of the optimization based approach are pointed out. Therefore a scenario for hopping as well as up-righting from every non-nominal face is shown. These results are not final results in sense of the mission yet, as asteroid modeling and parameter setting are still work in progress and will be enhanced while approaching Ryugu till 2018.

5.1 Hopping

For hopping the main objective has been to achieve an as far as possible relocation distance to cover larger areas on Ryugu. This distance is therefore divided into two objectives: The jumping distance up to the first impact δ on the soil and the final distance $\delta_{\max}$. Thereby the first impact distance is weighted higher, as it is the more reliable result. This is due to the excessive amount of bouncing, occuring due to low gravity and rotational energy stored in the lander itself, which is then transferred into translational energy at every impact. Thus the final distance is mainly used to evaluate the radius of a circle in which MASCOT will most likely come to rest, but not to evaluate a final position as such, because every hit decreases the accuracy of the prediction.
As MASCOT's survival time is limited by the battery charge another constraint, compiled into an objective, is the time $t(\delta^z_{\max})$ needed to reach an equilibrated state. This time is minimized in order to enable the highest time for scientific output and to lower the amount of locomotion time due to bouncing. Furthermore the maximum jumping height $\delta_{\max}$, as well as the maximum velocity in $\vec{e}_z$ are minimized and another constraint objective ensures, that velocity $\vec{v}_z$ in $\vec{e}_z$ is always safely lower than 0.5 times the escape velocity v_{esc}.
Thus the objective and constraints are:

$$J = \left\{ \delta^{-1}, \delta^{-1}_{\max}, t(\delta_{\max}), \delta^z_{\max}, |\vec{v}_z| \right\}_{\mathrm{v}} \tag{5}$$

$$J_{\mathrm{C}} = \left\{ |\vec{v}_z| < 0.5 \cdot v_{\mathrm{esc}} \right\}_{\mathrm{v}} \tag{6}$$

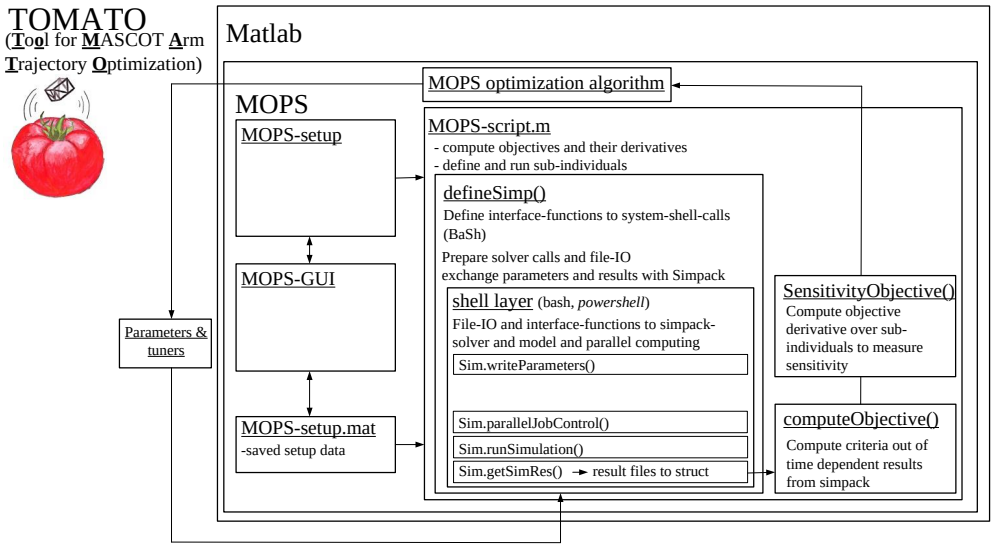

Figure 5. : Overview of the framework TOMATO

The optimization has been carried out for face A and B (nominal and opposite face, largest faces of the box, see Fig.2) as starting faces. In order to improve the convergence of the optimization, it is carried out stepwise, first indentifying the two angles. This approach is based on the assumption, that certain parameter's choice is dependent on the optimal choice of other parameters. As a second step, the angles are held constant and suitable accelerations are to be found. Last the maximum rotational velocity is determined. For details on the approach and its verification refer to [5].

Fig.6 shows the results of the penultimate step for the four dimensional parameter space of the first two steps, illustrating all the individuals of the optimization run. As the result the jumping distance δ up to the first hitpoint is used. Two maxima concerning the angles are clearly visible, whereas one of them is a global maximum for the set conditions. Fig.7 shows the same points as in Fig.6, but with the focus on the accelerations instead of the angles. Thereby it is shown, that for certain ranges of the arm acceleration, there is low sensitivity on changes of the latter, but a clear maximum exists at 33.55 $\frac{\text{rad}}{\text{s}^2}$. For the deceleration, the results are showing a maximum plateau which is compliant to the basic assumption, that higher decelerations would result in higher forces and thus higher distances. Fig.8 shows the influence of the last step - tuning of the maximum velocity. As already shown for the deceleration, the expected result is also shown by the optimization: increasing rotational velocity increases the energy stored in the system and thus results in larger jumping distances. As an additional result, the equilibrated total jumping distance is shown (the range of the y-axis is shrinked) to illustrate that an increase in input energy also increases the range of possible end positions and thus decreases the accuracy of the prediction. In the figures 9 and 10 the parabola of the first jump (blue) and the subsequent

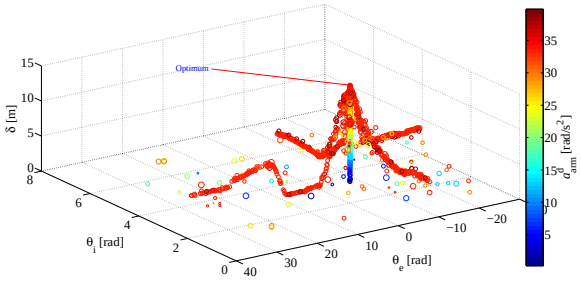

Figure 6. : Results on hopping distance up to the first impact in four dimensional parameter space for starting on face A cf. [13]; Marker size denotes maximum arm acceleration

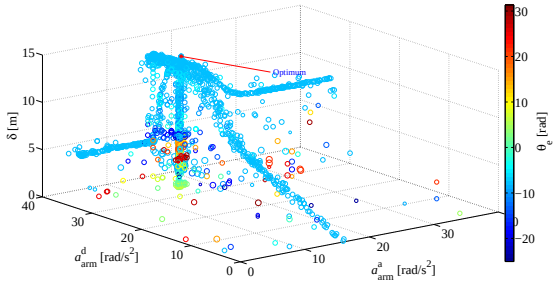

Figure 7. : Results on hopping distance up to the first impact in four dimensional parameter space for starting on face A cf. [13]; Marker size denotes initial angle of the arm

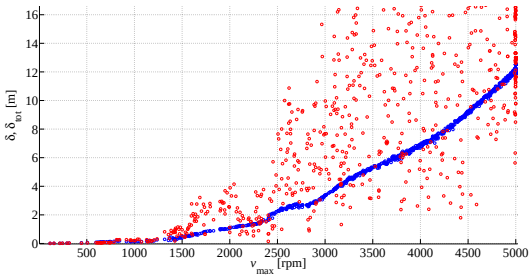

Figure 8. : Results on hopping distance up to the first impact and final position dependent on maximum rotational velocity of the mobility arm for starting on face A cf. [13]

hit points (red) of the simulation are shown. The green circle illustrates the circle in which MASCOT's end position is most likely situated. Thereby Fig.9 shows the best manually tuned trajectory, which has been chosen using common engineering assumptions, whereas Fig.10 denotes the optimized trajectory using the proposed approach. By comparing the two plots a factor of ≈ 6 can be evaluated for the increase in distance up to the first hit point and an even larger factor for the final equilibrium position. Nevertheless the longer equilibrated jumping distance also means larger uncertainty of MASCOT's final position. As a second case to verify the abilities

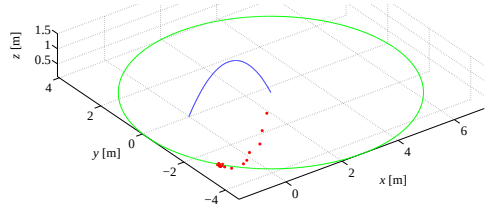

Figure 9. : Best manually tuned trajectory, blue parabola denotes first jump, red dots are subsequent hitpoints during bouncing for starting on face A cf. [13]

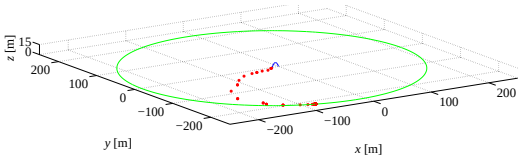

Figure 10. : Optimized hopping trajectory, blue parabola denotes first jump, red dots are subsequent hitpoints during bouncing for starting on face A cf. [13]

of the algorithm, jumping from face B has been used, as the case is not perfectly symmetric to case A. Therewith it has been checked if on one hand similar dependencies are found and if on the other hand parameters like the arm angles are sufficiently different from the face A solution. Fig.11 shows that the response surface, as well as the way through parameter space for the acceleration values is in general agreement with the ones of face A. Additionally it can be seen, that a more clearly visible maximum exists. In Fig.12 similar qualitative behaviour like in Fig.7 is visible, but with significantly different quantitative results on the optimal angles.

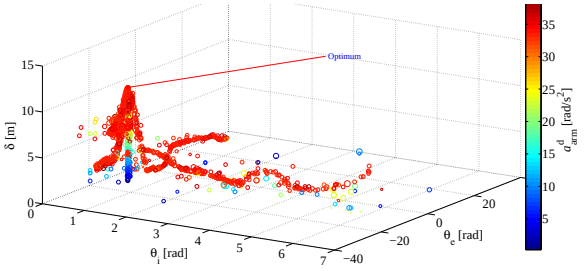

Figure 11. : Results on hopping distance up to the first impact in four dimensional parameter space for starting on face B; Marker size denotes maximum arm acceleration

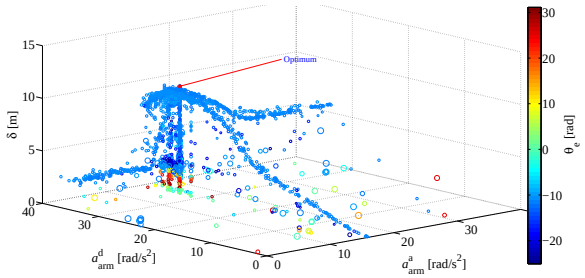

Figure 12. : Results on hopping distance up to the first impact in four dimensional parameter space for starting on face B; Marker size denotes initial angle of the arm

5.2 Up-righting

So called up-righting is the motion bringing MASCOT from any non-nominal face to the nominal measurement face A, as most of the scientific instruments are only able to measure in this position. Dependent on which face MASCOT lands on, manual solutions can be found more or less easily: e.g. for the faces E and F the rotation axis of the mobility unit points in normal direction of the soil, which is the most problematic condition. Due to soil friction and its anisotropic behaviour it is possible to up-right MASCOT from face E and F nonetheless, however with lower probability to equilibrate on face A. Fig.13 divides the solutions which landed on face A (Θ_A=1) from the non-successful cases. By the scattered pattern of successful up-rights it can be seen, that finding suitable solutions is not a trivial task, moreover if robust solutions are desired.

The main objective for up-righting is to minimize the face-membership-function Ξ_F, which rates each equilibrium

Table 1. : Variation ranges for the environmental and mobility parameters of sub-individuals

Case	μ_h	ε_r	E [MPa]	ω_{max}	a^d_{arm}
(1-3)	[0.7; 1.2]	-	-	-	-
(4-6)	-	[0.1; 0.6]	-	-	-
(7-8)	-	-	[0.1; 1]	-	-
(9-10)	-	-	-	$[0.9; 1] \cdot \omega^{des}_{max}$	$[1; 1.1] \cdot a^{d,des}_{arm}$

orientation based on its severity for the mission. Thereby face A results in the lowest values, followed by equal values for face C and D. Face B features slightly higher values, as up-righting from this face requires higher input energy and thus takes longer than from faces C and D. Worst cases are faces E and F as mentioned above. Additionally equilibrating time $t(\delta_{max})$, jumping distance

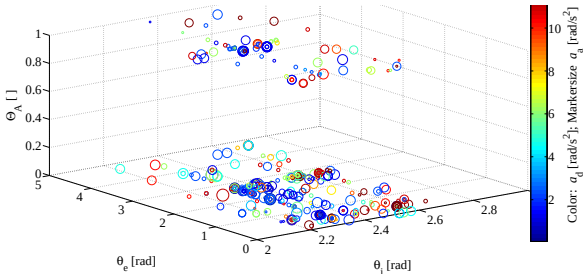

Figure 13. : Results on up-righting from face C, Θ_A is the membership function to evaluate if the final face is face A

δ_{max} and height δ^z_{max}, as well as velocity in $\vec{e}_z$ are minimized. Else the same escape velocity constraint as for hopping applies.

$$J = \left\{ \Xi_F, \delta, \delta_{max}, t(\delta_{max}), \delta^z_{max}, |\vec{v}_z|, \omega_{max} \right\}_v, \|\nabla J_k\|_1 \quad (7)$$

$$J_C = \left\{ |\vec{v}_z| < 0.5 \cdot v_{esc} \right\}_v \quad (8)$$

Furthermore for up-righting the sub-individual based robust optimization applies. Table 1 shows the ranges for the ten sub-individuals, which vary soil and actuation parameters and thus model inaccuracy in the current knowledge on the asteroid and unlikely system errors. The ranges are chosen such, that worst cases - most likely worse than what is to expect on Ryugu - are used to verify the applicability of the algorithm. Based on the ten cases the derivatives of the objectives are evaluated in order to rate the sensitivity as well. For final mission value optimization, more than ten cases may be used. As post-optimization check, a verification of the qualitative motion behaviour for up-righting is carried out. As the main result of the campaign, using optimized, robust trajectories MASCOT was able to up-right from every non-nominal face to face A in ten out of ten cases. Before optimization, up-righting from face E and F was not possible in every case and none of the trajectories were robust against bigger changes in environmental conditions. Additionally none of the solutions violated the escape velocity constraints and the settling time decreased from $\approx 800 - 900$ s before optimization to ≈ 300 s after optimization. The only case that took ≈ 500 s has been face E to face A, for which an even better trajectory will be found in prolonged optimization runs in future work. In order to illustrate the achieved goal of up-righting and additionally to underline that reasonable trajectories are found, Fig.14 shows a picture series of the up-righting process for starting face B, C and F. Hence all levels of difficulty are present in the visualized results and it can be seen, that no additional bouncing on non-nominal/intermediate faces is occuring.

6 CONCLUSION

In this article an optimization based technique to determine suitable arm trajectories for the asteroid lander MASCOT has been proposed. Using this approach trajectories for both, hopping and up-righting have been optimized successfully. Thereby the performance of the results goes far beyond the results of manual tuning, while being a fully automated process. For hopping longer jumping distances were achieved in order to allow planetary science to cover larger areas of the asteroid. Especially for up-righting robust solutions for a wide variety of soil parameters as well as unlikely actuator control inaccuracies were found. Thereby ten out of ten cases for up-righting from any non-nominal face are achieved, while even decreasing the settling time of the lander and thus enhancing the time for planetary science. The results for the intermediate specimen of the evolutionary strategies may also be used to analyze influences of the tuner parameters as well as to be treated as training data for operations.
Nevertheless the approach still has limitations: genetic algorithms need a sufficiently large number of specimen and generations to find suitable solutions, thus optimization runs need at least one week on nowadays powerful workstations, even though multi-threading using 20 cores is applied. Even though this runtime is still sufficiently fast to be able to update the trajectories once final information on Ryugu is gathered before the last data upload.

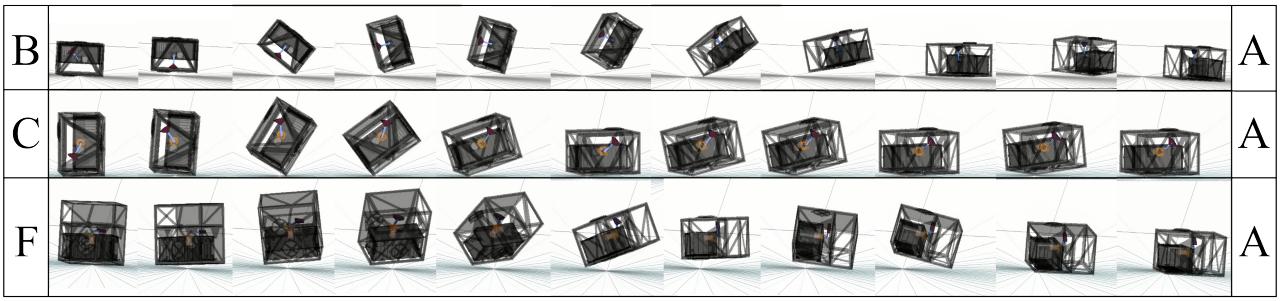

Figure 14. : Optimized up-righting motion in nominal case for face B, C and F; motion is completed within ≈ 300 s

For further work, the asteroid model as well as the system model will be farther enhanced as knowledge is gained approaching Ryugu. Thereby further optimization runs will step by step refine the trajectories aiming for the final set used during the mission after descent.

Acknowledgment

Special thanks are going to the main author's sister Pia Lichtenheldt who designed the logo for the framework TOMATO.

References

[1] Ulamec, S. et al.: Rosetta Lander - Landing and operations on comet 67P/Churyumov-Gerasimenko, Acta Astronautica, Elsevier, DOI: 10.1016/j.actaastro.2015.11.029, ISSN 0094-5765, 2015.

[2] Ho, T.-M. et al.: The Development and first Cruise Activity of the MASCOT Lander onboard the Hayabusa 2 mission Low-cost Planetary Mission Conference, Berlin, 2015

[3] Reill, J.; Sedlmayr, H.-J.; Neugebauer, P.; Maier, M.; Krämer, E.; Lichtenheldt, R.: MASCOT Asteroid Lander with Innovative Mobility Mechanism, 13th Symposium on Advanced Space Technologies in Robotics and Automation (ASTRA), ESA/ESTEC, Noordwijk, Netherlands, May 2015.

[4] Joos, H.-D.; Bals, J.; Looye, G.; Schnepper, K.; Varga, A.: A multi-objective optimisation-based software environment for control systems design, IEEE International Conference on Control Applications and International Symposium on Computer Aided Control Systems Design, Glasgow, Scotland, UK, pp. 7-14, 2002

[5] Lichtenheldt, R.; Schäfer, B.: Hammering beneath the Surface of Mars - Modellbildung und Optimierung des HP3-Mole in L. Zentner (Ed.): 10. Kolloquium Getriebetechnik, pp.169-186, ISBN 978-3-86360-065-5, Ilmenau, 2013

[6] Reill, J. et al.: Development of a mobility drive unit for low gravity planetary body exploration, 12th Symposium on Advanced Space Technologies in Robotics and Automation (ASTRA), ESA/ESTEC, Noordwijk, Netherlands, May 2013.

[7] Herrmann, F.; Kuß, S.; und Schäfer, B.: Mobility Challenges and Possible Solutions for Low-gravity Planetary Body Exploration. 11th Symposium on Advanced Space Technologies in Robotics and Automation: ASTRA 2011, 12. - 14. April 2011, Noordwijk, the Netherlands

[8] Lange, M.; Mierheim, O.; Hühne, C.: MASCOT - Structures design and qualification of an "organic" mobile pander platform for low gravity bodies . Proceedings of the 13th European Conference on Spacecraft Structures, Materials & Environmental Testing, 2014

[9] Iwashita, K.; Oda., M.: Mechanics of Granular Materials: An Introduction. Balkema, Rotterdam, Netherlands, S. 356, 1999

[10] Lichtenheldt, R.: A novel systematic method to estimate the contact parameters of particles in discrete element simulations of soil 4th International Conference on Particle-based Methods - Particles 2015, ISBN:978-84-944244-7-2, Barcelona, 2015

[11] Lichtenheldt, R.; Schäfer, B.; Krömer, O.: Hammering beneath the surface of Mars - Modeling and simulation of the impact-driven locomotion of the HP3-Mole by coupling enhanced multi-body dynamics and discrete element method Shaping the future by engineering: 58th Ilmenau Scientific Colloquium IWK, 2014

[12] V. Guibout; D.J. Scheeres: Stability of Surface Motion on a Rotating Ellipsoid, Celest. Mech., 87: 263-290, 2003

[13] Lichtenheldt, R.; Spytek, J.; Reill, J.: Coaching Mascot for broad-jumping: Multi-criterial optimization of the arm trajectories for Mascot's hopping locomotion 11th Low-cost Planetary Mission Conference, Berlin, 2015